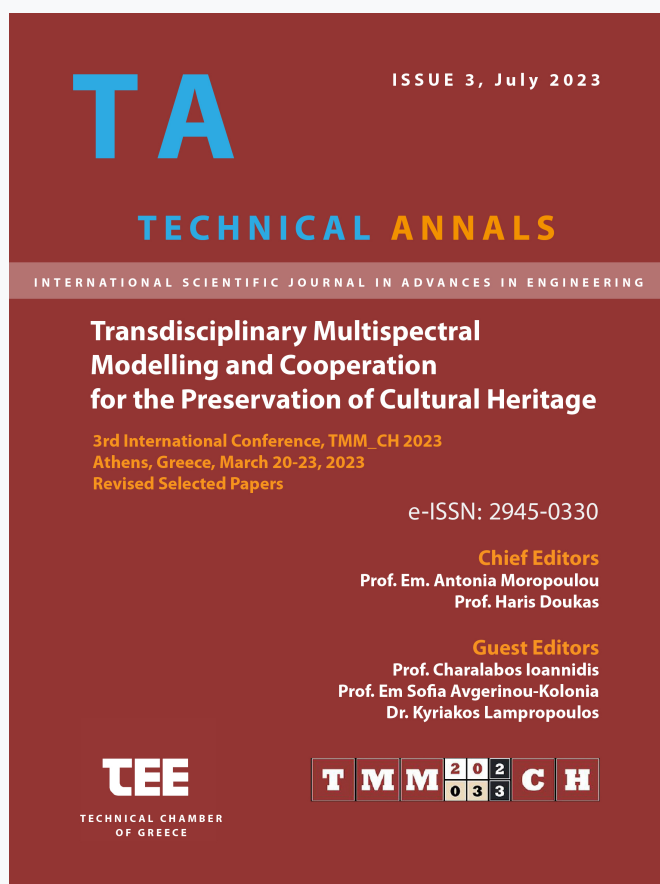


## Technical Annals

Vol 1, No 3 (2023)

Technical Annals



### Seismic-Energy Combined Retrofit Systems of Historical Buildings

*Ubaldo Saracco, Emilia Meglio, Antonio Formisano*

doi: [10.12681/ta.34801](https://doi.org/10.12681/ta.34801)

Copyright © 2023, Ubaldo Saracco, Emilia Meglio, Antonio Formisano



This work is licensed under a [Creative Commons Attribution-NonCommercial-ShareAlike 4.0](https://creativecommons.org/licenses/by-nc-sa/4.0/).

### To cite this article:

Saracco, U., Meglio, E., & Formisano, A. (2023). Seismic-Energy Combined Retrofit Systems of Historical Buildings: The Use of Light Metal Exoskeletons. *Technical Annals*, 1(3). <https://doi.org/10.12681/ta.34801>

# Seismic-Energy Combined Retrofit Systems of Historical Buildings: The Use of Light Metal Exoskeletons

Ubaldo Saracco<sup>1</sup>[0000-0002-1632-2122], Emilia Meglio<sup>1</sup>[0000-0003-4430-0876]  
and Antonio Formisano<sup>1</sup>[0000-0003-3592-4011]

<sup>1</sup>Department of Structures for Engineering and Architecture,  
School of Polytechnic and Basic Sciences,  
University of Naples "Federico II", P. le V. Tecchio 80, 80125 Naples, Italy  
emilia.meglio@unina.it, u.saracco@gmail.com,  
antoform@unina.it

**Abstract.** The current trend in retrofitting existing buildings is mainly seen under the environmental aspect, giving little attention to seismic issues. Contrary, recent European Union's policies in this field are based on integrated approaches aimed at improving both energy and earthquake performances. Therefore, the so-called seismic coats have been launched on the building market. In this framework, the design of a new system for seismic-environmental requalification of existing constructions made of masonry or reinforced concrete is presented and illustrated in the present paper through the application of a cold-formed steel framed structure. This system is provided with both insulation panels, used to provide energy benefits, and a X-bracing system, employed to absorb part of the seismic forces to preserve the existing structure from damage. In the current research work, firstly, a description of the coat's components is presented. Secondly, the anti-seismic solution has been used to reinforce RC frames and its effectiveness has been proved by refined mechanical analyses in the non-linear field. Finally, the comparison of performances of examined structural system before and after the intervention has been made to evaluate the benefits provided by the proposed coating system under a seismic viewpoint.

**Keywords:** Seismic upgrading, Seismic-Energy Coat, RC frame, Light Exoskeletons, Cold-Formed Steel.

## 1. Introduction

Italian legislation identifies two main interventions to be executed for increasing seismic performances of buildings: upgrading interventions, when the seismic safety factor  $\zeta_E$ , intended as the capacity acceleration over the demand acceleration ratio, augments of at least 0.10, and retrofitting interventions, when the  $\zeta_E$  factor assumes unitary value as per new constructions. Multiples are the types of interventions to be executed and they differ from each other based on the typological and structural differences of the buildings they are designed to fit on [1][2][3][4]. Their proven validity derived from

years of scientific tests and applications showing good results in applicability and flexibility of use. It is clear that the study of new techniques must first pass through test and evaluation phases. The retrofit of existing structures strongly depends on their degree of damage, which can be attributed to age, corrosive actions, material or anthropogenic degradation, etc. For this reason, it is necessary to carry out experiments on a diversified pool of structures on which various types of interventions can be applied. Structures are often created from scratch with particular characteristics of simulated deterioration, which never perfectly correspond to the real state of a structure aged over time. The availability of structures already completed in an advanced state of decay would be a valuable opportunity for studying such retrofit interventions. In previous years, the European Community decided to reduce steel production and, as a consequence, many production plants were abandoned over time. In the Bagnoli area of Naples hosting the ILVA industrial complex, which extended over a densely populated, touristic area close to the coastline, production of steel was done. Therefore, it was one of the first production areas to be decommissioned and partially demolished. Part of the buildings located there were then subjected to protection restrictions, as they are evidence of the value of industrial engineering of the 60s and 70s. The remaining part of the built-up, purely made of reinforced concrete, were preserved for their precious use as "samples" on which to carry out tests and research, becoming a huge open-field research laboratory. Thus, the ILVA-IDEM (ILVA IntelligentDEMolition) [5] program was born in collaboration between the University of Naples Federico II and many participating subjects. Most of the RC structures placed in the ILVA area were built before 1980 when Naples was not yet considered seismic territory. Consequently, they were made of one-direction moment resisting frames, mainly designed to withstand gravity loads (Gravity Load Design - GLD). It must also be stated that for these RC structures, located close to both a highly industrial area and the sea, the atmospheric environment was highly harmful, leading to both corrosion damage to steel bars and concrete carbonation. This scenario is particularly suited for application of retrofit or upgrading interventions, since they would be evaluated on already degraded structures resulting from years of exposure to particularly aggressive environments. The current memory is framed in this context, focusing the attention on the use of a cold-formed steel framed exoskeleton for strengthening and stiffening an existing RC frame. This framed structure represents one of the sub-structures (modules) of the ILVA-IDEM building after cutting operation at floor levels. The reinforcing technique herein presented is the Resisto 5.9 system, a seismic-energy technological coating designed by the Progetto Sisma company, that improves both seismic performance and energy efficiency of existing masonry [6][7] and RC [6]. A 2D frame is selected from the modules of the 3D office building under exam and assessed with and without the proposed reinforcing system by means of two structural software, namely Abaqus and Pro\_Sap. The purpose of this evaluation is to study the contribution of the coating system for seismic upgrading of the structure. The first software, Abaqus, allows to precisely build the system with all its peculiarities, including connections and non-linear laws of materials, providing very accurate results. Contrary, Pro\_Sap is a commercial type of FEM software mainly used in the professional practice, that allows to perform seismic analyses on both new and existing structures. The aim of the work is to compare the output results deriving from the two

programs to highlight the capacity of the simpler software to effectively simulate the seismic behaviour of the investigated RC frame.

## 2. The structure under investigation

### 2.1 The Office Building

The original building was built in the 1970s and it served as an office complex (**Fig. 1**). A framed structure with brick infill walls, designed to resist only vertical loads, was built on two levels with overall plane dimensions of 41.60 m x 6.50 m and height of 6.60 m. It was made of a single bay in the transversal direction and 12 bays in the longitudinal direction (**Fig. 2**) [7][8][11].

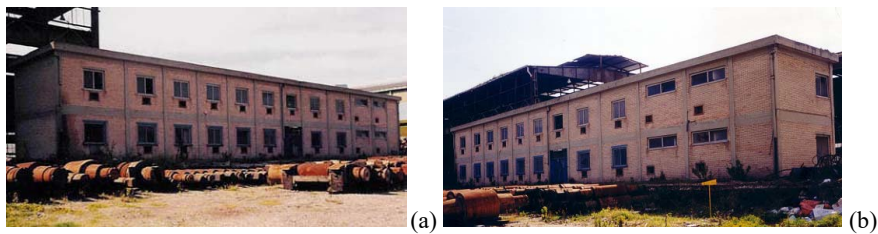


**Fig. 1.** Side view of the original building: north-east (a) and north-west (b) facades.

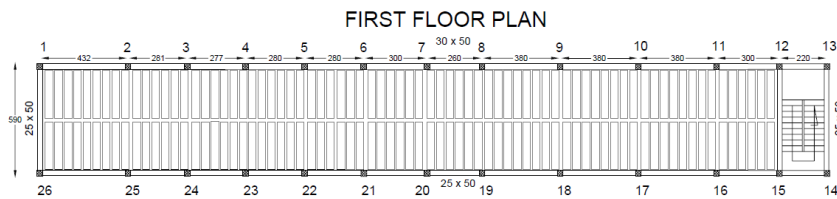


**Fig. 2.** Plan configuration of the building at the first level.

The structure was then stripped of the infill components, leaving only the bare frame with the 12 spans (**Fig. 3**). By cutting the beams at the floor levels, 6 modules were derived (**Fig. 4**). The first and sixth modules had different characteristics: the module n.1 consisted of three transverse column alignments and two unequal bays in the longitudinal direction, while the n.6 one was occupied by the staircase. Instead, the modules from the second to the fifth were the same in terms of geometry and structural elements.

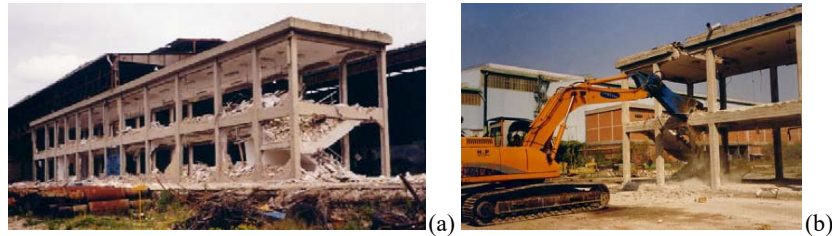


**Fig. 3.** Bare frame (a) and cutting of the floors for the definition of the structural modules (b).

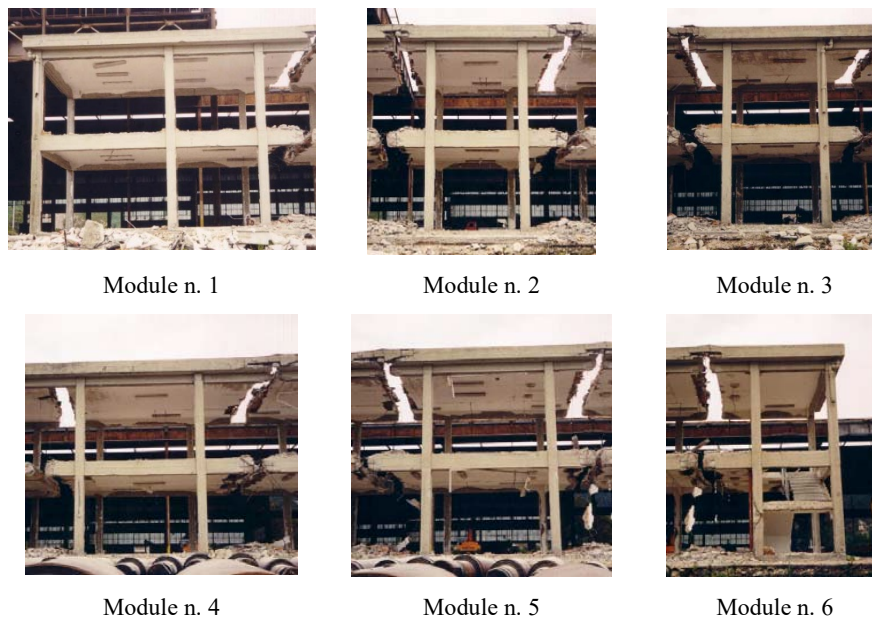


**Fig. 4.** Modules obtained from the infill demolition and floor cutting phases.

## 2.2 The Structural Module n.5

The analyses herein presented refer to the module n.5 (**Fig. 5**) of the built complex, which has been selected due to the homogeneity of characteristics with most of the building modules, except than those with numbers 1 and 6. The geometric configuration of this module is characterized by a rectangular shape measuring 6.30 x 5.90 m and developing on two storeys with heights of 3.55m and 6.81m at first and second floor, respectively. The thickness of the floor is 24 cm and 20 cm, respectively, at the first and second floors. Both floors have a central transverse joist and are supported, at the first level, by emerging rectangular beams (30 x 50 cm and 25 x 50 cm) placed along the longitudinal direction, while at the second level, the beams have a T cross-section of equal width and the same height of the first level beam members. In the transverse direction, the lateral resistance is essentially provided by the columns, which have a square section of 30 x 30cm and are reinforced with four longitudinal steel bars,  $\Phi 12$ ,

placed in the section corners. Stirrups  $\Phi 8$  are placed in the columns every 300 mm. The foundation structure is composed of two inverted T-beams placed in the longitudinal direction (**Fig. 7**).



**Fig. 5.** General view of the module n.5.

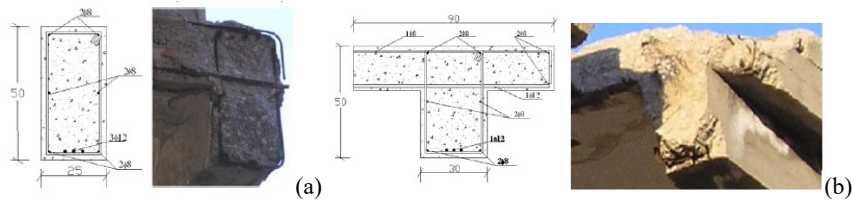


**Fig. 6.** Right side of beam sections at first (a) and second (b) level.

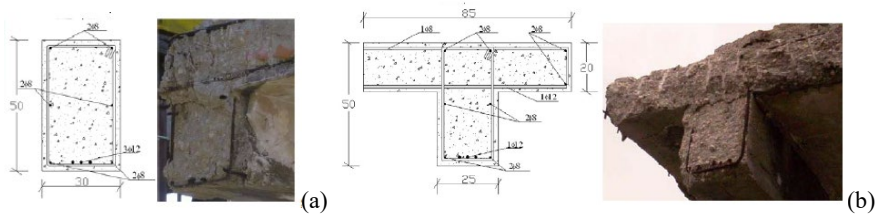


**Fig. 7.** Left side of beam sections at first (a) and second (b) level.

### 2.3 The Seismic-Energy Integrated Coat

The Resisto 5.9 system [5] is a technological coating solution allowing for the improvement of seismic performance of existing buildings, also combining their energy efficiency through the integrated insulating package (**Fig. 8**).

The reinforcement of the existing structure is performed by integrative steel structural elements collaborating on the surface. Particularly, the system is made up of steel elements suitably connected to each other and to the RC frame.

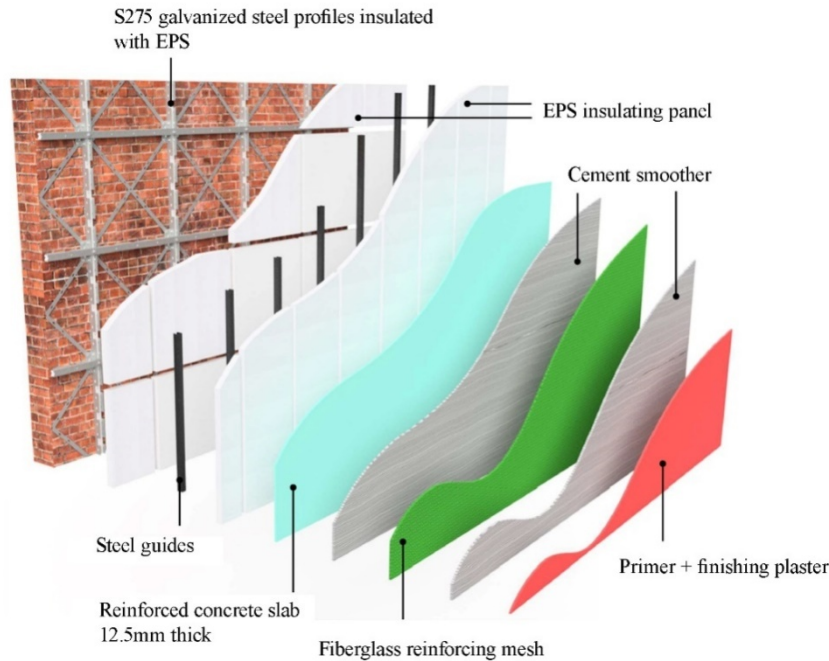


**Fig. 8.** Layers of the Resisto 5.9 system.

The metal profiles (**Fig. 9**) have a hollow rectangular cross-sections with dimensions of 60 mm x 40 mm and 50 mm x 25 mm and thickness of 3 mm. They are made of galvanized S275GD+Zsteel (yield strength  $f_y = 275\text{MPa}$  and failure strength  $f_u = 430\text{MPa}$ ). Three mm thick cold-formed plates with side length of 50 mm complete the system by acting as a connection between vertical and horizontal members and as an anchor point for the bracing. The elements are positioned in adhesion on the external surface of the wall, placed side by side and connected to the structure's surface through anchors with regular pitch. The anchoring must be of the chemical type, made by injection of a specific resin into holes of suitable diameter and depth and subsequent insertion of class 8.8 threaded steel rods. Each profile is connected to the adjacent one/s to ensure continuity of the reinforcing elements according to vertical, horizontal and bracing directions: shaped pre-galvanized steel plates allow for the union between profiles and bracings through class 8.8 galvanized steel bolts. From a structural point of view, the Resisto 5.9 system is aimed at the seismic upgrading/retrofit of buildings pursuant to sections 8.4.2 and 8.4.3 of the NTC 2018 standard [8], which deals with global interventions aiming at improving or retrofitting the entire structural organism. The system can also be used as a local intervention pursuant to section 8.4.1 of the NTC 2018 standard [8], which concerns interventions on single portions or single elements in order to contribute to the reduction of the structure vulnerability towards local mechanisms/kinematics. In this paper the effect that this system offers towards the seismic upgrading of an existing RC structure, without analyzing the energy issues evaluated in another context [4], is evaluated.

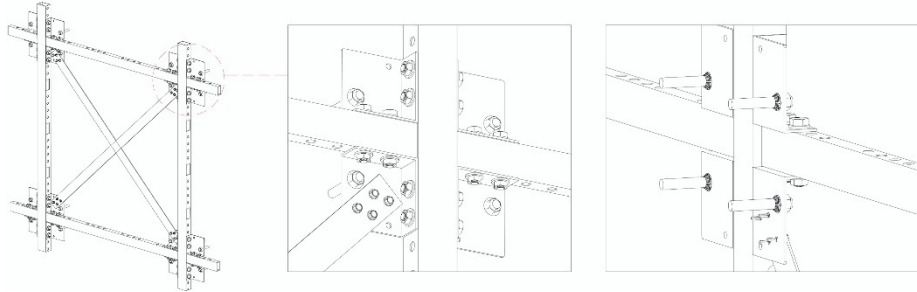


Fig. 9. Components of the Resisto 5.9 system.

#### 2.4 Framework of FEM Modeling

The modeling of the RC structure under examination was carried out with the aid of the softwares Abaqus and Pro\_Sap [9] [10] by creating a two-storey 2D frame model. The motivation of this choice is to be found in the research of the contribution of the Resisto 5.9 coating system on a 2D frame undisturbed by the dynamics of the rest of the structure. The RC frame, previously presented in this paper as module n. 5 (see 2.2), was submitted to non-linear static analyses with and without the seismic coating in order to evaluate the contribution in terms of seismic contribution provided by the reinforcement with the proposed system. Three structural models were built: a control frame without reinforcement (RC Frame), a reinforced frame with the seismic coat only linked to the RC structure (RC Frame + Resisto NOT Fixed) and a reinforced frame where the vertical members of the seismic coat are fixed to the foundation structures (RC Frame + Resisto Fixed). To make a more realistic comparison between the two softwares, in Pro\_Sap it was decided to model only the first level of the reference frame where seismic forces are experimentally applied. For this reason, the presence of the upper floor was considered by applying equivalent concentrated loads at the head of the columns, as presented in Section 4.4. To obtain objectively correct results deriving from different modelling approaches through the two used programs, it is necessary to start from input data compatible with the state of the materials being analyzed. For this reason, reference to the experimental mechanical characterization of structural materials was done considering in the FEM models the measurement units shown in **Table 1**.

Table 1. Measurement units of the International System.

| SI (mm) |   |                            |   |                          |                         |                       |
|---------|---|----------------------------|---|--------------------------|-------------------------|-----------------------|
| mm      | N | tonne (10 <sup>3</sup> kg) | s | MPa (N/mm <sup>2</sup> ) | mJ (10 <sup>-3</sup> J) | tonne/mm <sup>3</sup> |

#### 2.5 Mechanical Characterization of Materials

The investigations on materials carried out on the structural RC module under examination are part of the whole mechanical characterization performed within the ILVA-IDEM project [3], which saw destructive and non-destructive tests to obtain the necessary information on concrete and steel samples extracted from the members (Fig. 10).



The use of several samples allows to derive the average resistances of the various structural materials which were subsequently used as mechanical parameters in the numerical analyses carried out (**Table 2** and **Table 3**) [11].



**Fig. 10.** Extraction of cylindrical cores from module n.6.

**Table 2.** Concrete samples' mechanical properties.

| Specimens<br>n. | Unit weight<br>(kg/m <sup>3</sup> ) | Elastic modulus<br>(MPa) | Strength<br>(MPa) |
|-----------------|-------------------------------------|--------------------------|-------------------|
| 1               | 2244                                | 17692.0                  | 20.5              |
| 2               | -                                   | 16666.7                  | 21.0              |
| 3               | 2235                                | 16129.2                  | 19.9              |
| Average         | 2239                                | 16829.3                  | 20.5              |

**Table 3.** Rebar samples' mechanical properties.

| Specimens<br>n. | Φ<br>(mm) | Length<br>(mm) | Yielding<br>load<br>(kN) | Ultimate<br>load<br>(kN) | Ultimate<br>stress<br>(MPa) | Yielding<br>Stress<br>(MPa) |
|-----------------|-----------|----------------|--------------------------|--------------------------|-----------------------------|-----------------------------|
| 1               | 8         | 1040           | 29.0                     | 33.0                     | 656.5                       | 576.9                       |
| 2               | 8         | 975            | -                        | 41.0                     | 815.7                       | -                           |
| 3               | 8         | 500            | 23.1                     | 33.4                     | 664.5                       | 459.6                       |
| Average         |           |                |                          |                          | 712.2                       | 518.25                      |
| 4               | 10        | 558            | 39.5                     | 59.2                     | 753.8                       | 502.9                       |
| 5               | 10        | 520            | 38.9                     | 58.8                     | 748.7                       | 495.3                       |
| 6               | 10        | 485            | -                        | 62.7                     | 798.3                       | -                           |
| Average         |           |                |                          |                          | 766.9                       | 499.1                       |
| 7               | 12        | 850            | 44.1                     | 73.8                     | 652.5                       | 389.9                       |
| 8               | 12        | 570            | 53.1                     | 82.2                     | 726.8                       | 469.5                       |
| 9               | 12        | 860            | 53.0                     | 79.0                     | 698.5                       | 468.6                       |
| Average         |           |                |                          |                          | 692.6                       | 442.7                       |

The recording of experimental data on materials serves to calibrate the mathematical model to ensure correct monitoring of the interventions to be performed. In this framework, the absence of an adequate degree of knowledge can lead to considerable variations in the results, as evidenced in [12] and [13]. Therefore, in order to implement a

valid theoretical model of the substructures under study, the National Seismic Service of the Civil Protection Department, in collaboration with the University of Chieti/Pescara, performed dynamic tests on the structure with modal identification and subsequent calibration of results in the FE model of the module to test the reliability of the mechanical characterization [14]. In the following the mechanical parameters of materials used for modelling the RC module in the Abaqus CAE and Pro-Sap programs are reported.

**Abaqus Mechanical Parameters.** The data obtained from the analyses conducted on the structural samples under examination led to the definition of the mechanical parameters necessary to accurately model the non-linear behavior of the materials. The data tables related to each material are shown below. In particular, a Concrete Damage Plasticity model was used for the concrete (**Table 4**), which is based on the formulations regarding the yield functions proposed by Lubliner et al. [15]. To define B450C steel of rebars, data from tests carried out on site specimens were entered (**Table 3**). The properties of steel members of the Resisto 5.9 coating system were defined in **Table 5**.

**Table 4.** Concrete’s mechanical parameters.

| <b>Density</b>                    |                         |                 |            |                               |
|-----------------------------------|-------------------------|-----------------|------------|-------------------------------|
| Mass Density                      | 2.239E-009              |                 |            |                               |
| <b>Elastic</b>                    |                         |                 |            |                               |
| Young’s Modulus<br>10000          | Poisson’s Ratio<br>0.18 |                 |            |                               |
| <b>Concrete Damage Plasticity</b> |                         |                 |            |                               |
| Dilation Angle<br>40              | Eccentricity<br>0.1     | Fb0/fc0<br>1.16 | k<br>0.667 | Viscosity Parameter<br>0.0001 |
| <b>Tensile Behaviour</b>          |                         |                 |            |                               |
| Yield Stress<br>1.1               | Fracture Energy<br>0.6  |                 |            |                               |

**Table 5.** Mechanical properties of the Resisto 5.9 system steel members.

| <b>Density</b>             |                             |
|----------------------------|-----------------------------|
| Mass Density               | 7.85E-009                   |
| <b>Elastic</b>             |                             |
| Young’s Modulus<br>210000  | Poisson’s Ratio<br>0.3      |
| <b>Plastic</b>             |                             |
| Yield Stress<br>275<br>430 | Plastic strain<br>0<br>0.19 |

**Pro\_Sap Mechanical Parameters.** According to on site-inspections, the concrete has a compressive strength of 24.8 N/mm<sup>2</sup> (**Fig. 11a**), steel rebars for concrete have a yielding strength of 450 N/mm<sup>2</sup> (B450C) and steel of the Resisto 5.9 system’s profiles has a yielding strength of 275 N/mm<sup>2</sup> (**Fig. 11b**).

| Identifying string   | Existing concrete                 | Identifying string   | Steel Fe430 - S275                |
|--|-----------------------------------|--|-----------------------------------|
| <b>General data</b>  |                                   | <b>General data</b>  |                                   |
| <input checked="" type="checkbox"/> Existing material                |                                   | <input type="checkbox"/> Existing material                           |                                   |
| FC confidence factor m   | 1.0                               |  |                                   |
| FC confidence factor r   | 1.0                               |  |                                   |
| <b>Strengths</b>   |                                   | <b>Strengths</b>   |                                   |
| Strength Rcm   | 248.0 [daN/cm <sup>2</sup> ]      | Strength ftk   | 4300.0 [daN/cm <sup>2</sup> ]     |
| Strength fctm  | 22.65 [daN/cm <sup>2</sup> ]      | Strength fyk   | 2750.0 [daN/cm <sup>2</sup> ]     |
| <input checked="" type="checkbox"/> Elastic-plastic for non linea... |                                   | Strength fd  | 2750.0 [daN/cm <sup>2</sup> ]     |
|  |                                   | Strength fd (>40)  | 2500.0 [daN/cm <sup>2</sup> ]     |
|  |                                   | Allowable stress   | 1900.0 [daN/cm <sup>2</sup> ]     |
|  |                                   | Allowable stress (>40)   | 1700.0 [daN/cm <sup>2</sup> ]     |
|  |                                   | <input checked="" type="checkbox"/> Elastic-plastic for non linea... |                                   |
| <b>Property</b>  |                                   | <b>Property</b>  |                                   |
| Sp. weight   | 2.2390e-03 [daN/cm <sup>3</sup> ] | Sp. weight   | 7.8500e-03 [daN/cm <sup>3</sup> ] |
| Thermal expansion  | 1.0000e-05 [1/C]                  | Thermal expansion  | 1.2000e-05 [1/C]                  |
| Damping  | 5.0                               | Damping  | 5.0                               |
| <b>Elastic constants</b>   |                                   | <b>Elastic constants</b>   |                                   |
| E modulus  | 100000.0 [daN/cm <sup>2</sup> ]   | E modulus  | 2100000.0 [daN/cm <sup>2</sup> ]  |
| Poisson  | 0.18                              | Poisson  | 0.3                               |
| G Modulus  | 42373.0 [daN/cm <sup>2</sup> ]    | G Modulus  | 807690.0 [daN/cm <sup>2</sup> ]   |

**Fig. 11.** Materials implemented in the Pro\_Sap software: existing concrete (a) and steel of the seismic coat elements (b).

### 2.6 Modeling Process in Abaqus CAE

The modeling of the three-dimensional elements facing the structure under examination was carried out using the "part" command of the Abaqus CAE software. The concrete elements were modelled as homogeneous solid elements (Fig. 12a), while longitudinal rebars and stirrups were modelled as beam elements with their proper cross-sections. Finally, the cold-formed steel parts of the Resisto 5.9 coat were modelled through "shell" elements by assigning the relative thickness to each section (Fig. 12b and c). After individual elements of both the RC structure and the coating system were modelled, by using the "assembly" module of the program the entire model was constructed putting each element in the right position thanks to the translate and rotate commands (Fig. 13).

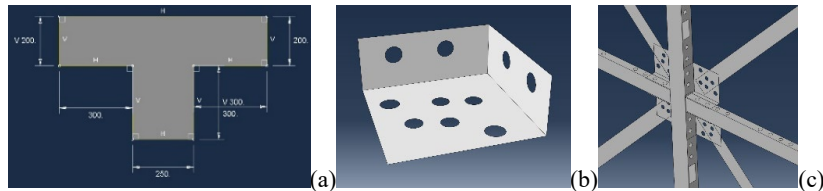


**Fig. 12.** Dimensions of the RC T beam (a), the Resisto 5.9 gusset plate (b) and 3D view of the bracing system of the coating system (c).

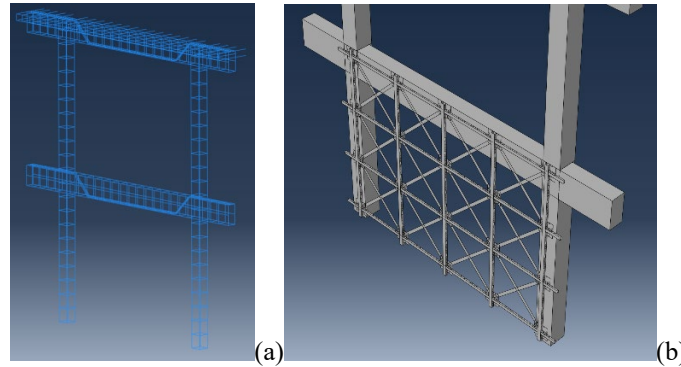


**Fig. 13.** Assembly of rebar and stirrups of the RC structure members (a) and the Resisto 5.9 system mounted on the RC frame (b).

**Interactions and boundary conditions.** Once the model was assembled, the propaedeutic step for the analysis was the regulation of the interactions among elements together with assignment of constraint conditions. Abaqus is not able to understand automatically the interaction among elements; for this reason, these interactions, such as for example the "embedded" interaction between the RC members and their rebars, were defined in the program. These constraints regulate the symbiotic behaviour of steel and concrete by simulating perfect adherence between the two materials (**Fig. 14**). The subsequent interactions concerned the application of the exoskeleton on the RC frame and the relationships between the exoskeleton's components itself, such as braces, vertical members and horizontal ones. These last interactions were regulated by the "tie" command between gusset plates and members and between gusset plates and braces to simulate the behavior of a bolted connection without defects (**Fig. 14**).

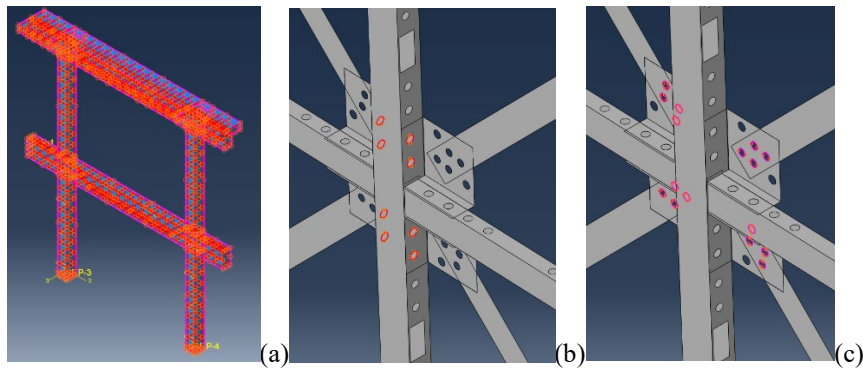


**Fig. 14.** Embedded rebars (a), tie between plate and members (b) and tie between plate and braces (c).

As for the boundary conditions, two conditions were set up: full restraints at the base of the pillars and gravitational loads on the floors (**Fig. 15a**). In the constraint conditions, a controlled displacement constraint was also set on the first level beam in order

to perform a controlled-displacement push-over analysis (**Fig. 15b**). No stress was applied to the exoskeleton of the Resisto coat, except than its own weight. This expedient makes possible to keep the analyses on the bare RC frame and the stiffened frame perfectly comparable to each other, so to read the upgrading done by the Resisto 5.9 system.

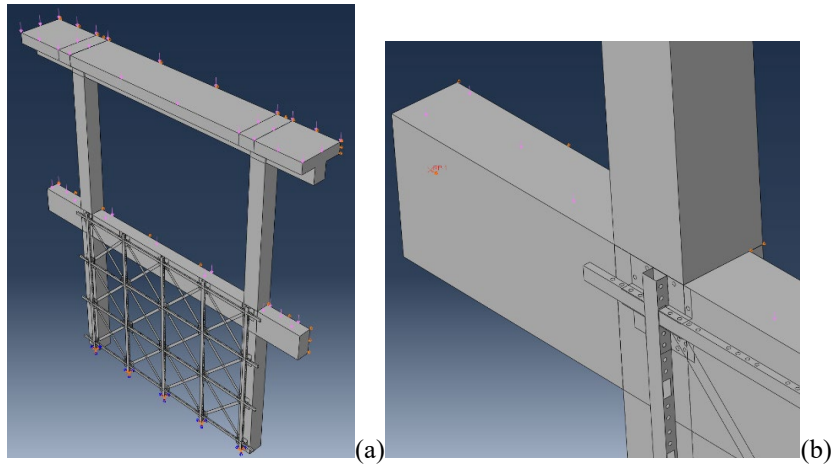


**Fig. 15.** Boundary conditions of the composite structure (a) and displacement applied to the C beam for pushover analysis purpose (b).

**Meshing.** A necessary phase for the correct analysis execution is the accurate choice of the mesh [16] [17]. The evaluations herein performed to define the optimal mesh, which were found to balance the best accuracy degree of results towards the elaboration time, are omitted for the sake of conciseness.

**Fig. 16** shows the difference in terms of mesh size among various elements, where the densest discretization was used in the Resisto 5.9 parts to have more detailed information on their behaviour.

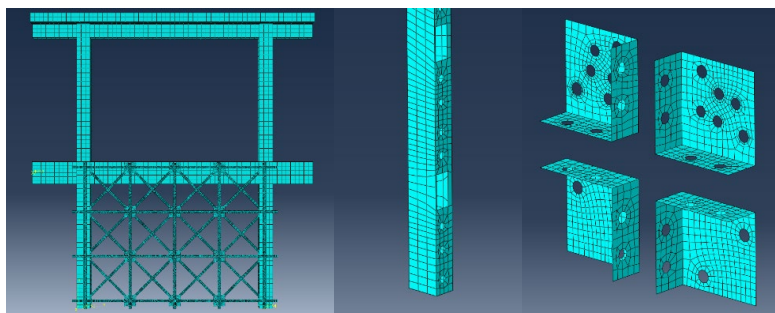


**Fig. 16.** Different components of the structure after meshing operation.

## 2.7 Modeling Process in Pro\_Sap

The model of the composite RC frame –coating system structure was also built in the Pro\_Sap finite element environment by implementing the geometrical and mechanical parameters already introduced in previous Sections 2.2 and 2.3. Leaving aside the detailed description of the elements constituting the system, as it was already introduced in the relevant section, in the following only the way they were implemented in the calculation software is shown.

Beams (25x50 cm cross-section) and columns (30x30 cm cross-section) of the RC frame were modelled as D2 elements, i.e. one-dimensional elements defined by two nodes, to which the property of non-linear beams were assigned. In all three models, fixed boundary conditions were assigned to the RC columns. Horizontal members (2.5x5 cm hollow rectangular cross-section with thickness of 3 mm) and vertical members (4x6 cm hollow rectangular cross-section with thickness of 3 mm) of the reinforcement system were modelled as D2 elements as well. They were placed one after another with a pitch of 1 m and were fixed at any intersection between RC columns and beams by means of 15 cm links having property of infinitely stiff material. The bracing diagonals (0.3x5 cm cross-section) were modelled as non-linear trusses resisting only to axial forces. A M3 node release was assigned to steel horizontal and vertical members to simulate the constraint conditions. Only in the third model (RC frame + Resisto 5.9 fixed at the base) fixed boundary conditions were assigned at the base of the vertical members. **Fig. 17** and **Fig. 18** show the solid and wireframe graphics, respectively, of the three FEM models under study.

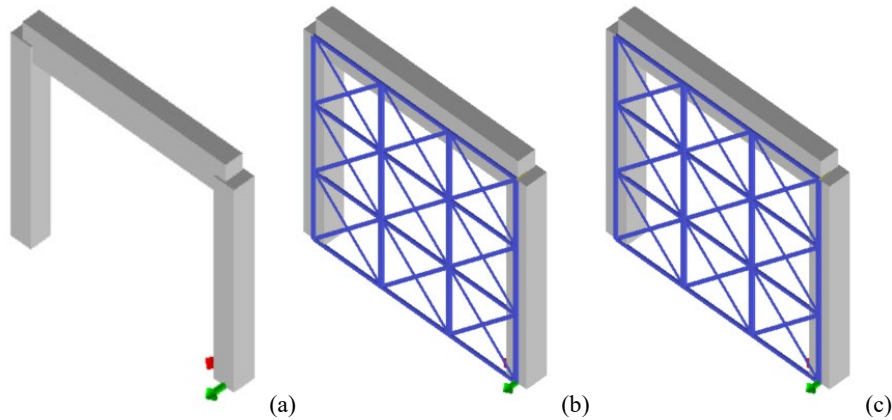


**Fig. 17.** Solidview of the three FEM models: RC Frame (a), RC Frame + Resisto NOT Fixed in Foundation (b) and RC Frame + Resisto Fixed in Foundation (c).

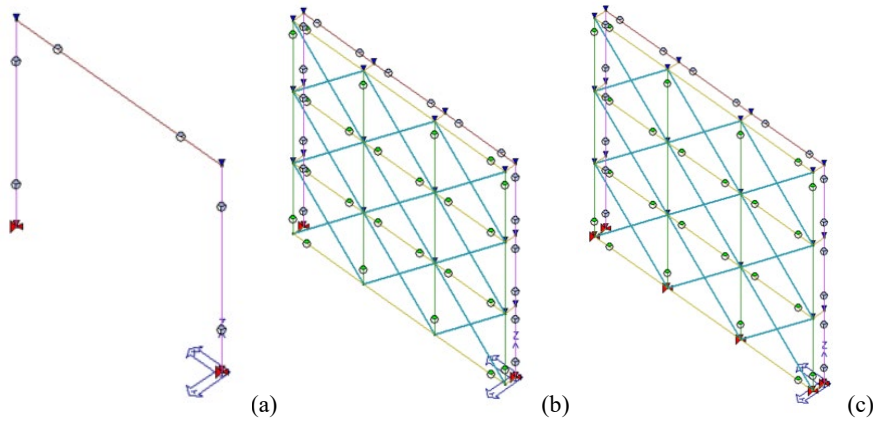


**Fig. 18.** Wireframe graphic of the three models: RC Frame (a), RC Frame + Resisto NOT Fixed in foundation (b) and RC Frame + Resisto Fixed in foundation (c).

Finally, loads were applied. Dead loads of the structural elements were automatically calculated by the software. The first floor load was manually applied as global distributed load on the RC beam with a value of 14.5 kN/m. The presence of the upper level of the RC frame was considered by applying a nodal load of 44.28 kN at the top of each column.

## 2.8 FEM models and seismic test on the bare RC frame

The three different FEM models already presented in Section 2.7 (RC Frame; RC Frame + Resisto NOT Fixed in Foundation; RC Frame + Resisto Fixed in Foundation) were tested under static non-linear analyses. As far as the push-over curves are concerned, the master joints to be monitored for plotting the capacity curve was chosen in the middle of the end cross-section of the first level beam. To compare the performance of different retrofit solution, the necessary first step was the analysis of the experimental data coming from the lateral test performed within the ILVA-IDEM campaign on the bare RC frame. This test was conducted adopting a cyclic loading history with variable load steps stopped before occurrence of any hinge in the RC members. Therefore, the diagram of **Fig. 19** shows only the trend of a foreseeable behavioral response of the frame having an initial branch determined experimentally and a subsequent perfectly plastic behaviour not investigated in the full-scale test.

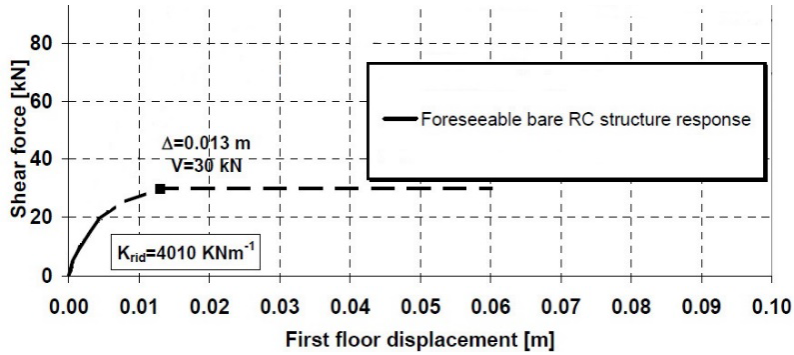


Fig. 19. Foreseeable structure response of the bare RC frame.

### 2.9 Abaqus CAE analysis results

From the analyses carried out with the ABAQUS program on the bare RC it can be seen that plastic hinges started when concrete degraded and they largely developed at a displacement of 5cm. Yielding of rebars starts at 3cm of displacement and was localized at both pillar bases, also extending to the areas corresponding to the nodes. The active yielding state of concrete and rebars is displayed in Fig. 20.

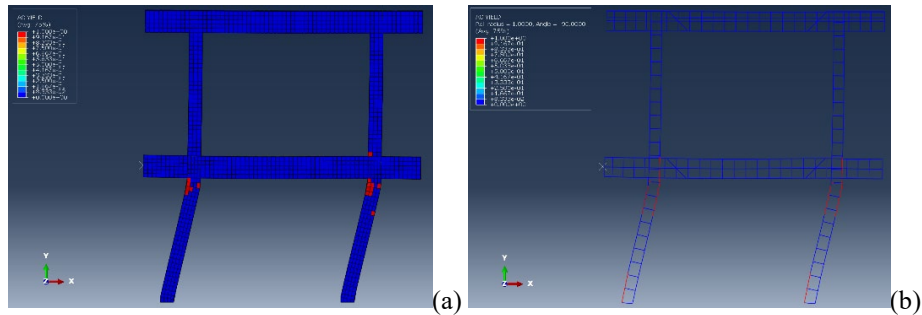
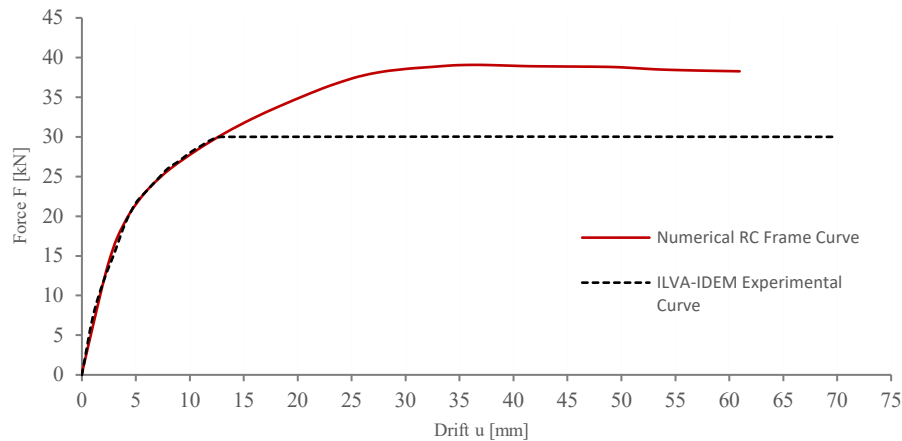


Fig. 20. Concrete(a) and rebar(b) active yield states.

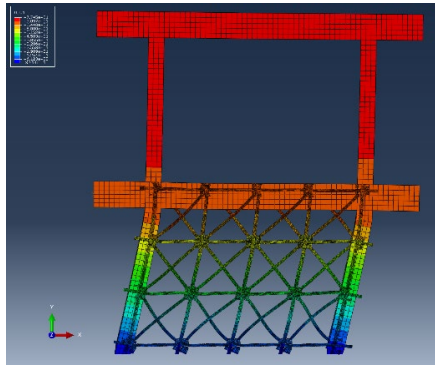
The curve obtained from pushover analysis is represented in Fig. 21, where it is compared with the experimental curve previously illustrated. It can be observed that the first branch of the numerical curve fits very well the initial branch of the experimental curve. This confirms the validity of the FEM model implemented, which can be therefore used for subsequent analyses aiming at retrofitting the studied bare RC frame.



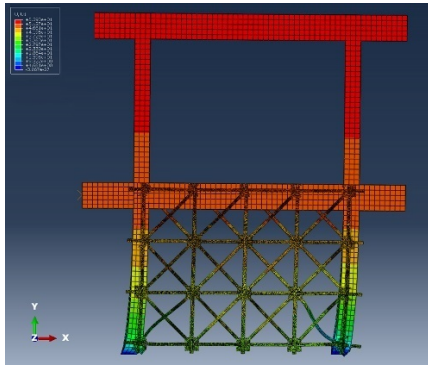


**Fig. 21.** Numerical and experimental pushover curves on the bare RC frame.

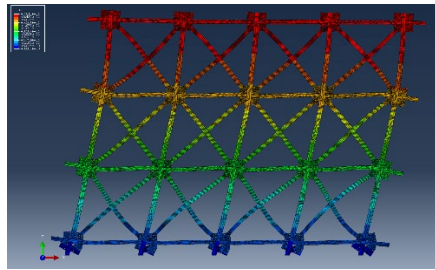
The Resisto 5.9 system allowed to reduce the distribution of stresses in the RC frame with an evident beneficial impact to increase the structural stiffness. This issue can be found in the distribution of active yielding state in the two different models (Resisto NOT Fixed in Foundation and Resisto Fixed in Foundation) compared to that of the bare RC frame. The Fixed model showed the greatest drift with the bracing system reaching yielding state (**Fig. 22e** and **g**). In this model, a displacement of 70 mm in the first storey beam was attained (**Fig. 22a**), while the non-Fixed model reached at the same point a displacement of about 50 mm (**Fig. 22b**). The drift obtained with the Resisto 5.9 system is also shown in **Fig. 22** Σφάλμα! Το αρχείο προέλευσης της αναφοράς δεν βρέθηκε. **c** and **d**, where it is noticed that in the fixed model the entire exoskeleton reached the largest drifts under lateral loads. In particular, the top end of the beam showed a displacement of about 51 mm. On the other end, the non-fixed model did not absorb a significant amount of load. In fact, few bracing elements reached the yielding point (**Fig. 22f** and **h**). In this case, the bottom end of the exoskeleton moved with the RC frame of about 35 mm, while the top end shifted of about 50 mm. This means that the differential displacement in the exoskeleton was about 15 mm. Finally, it should be noted that in the non-fixed model the analysis failed to converge at a displacement of about 40 mm because of an excessive deformation of the components. Nonetheless, this FEM model presented a different failure mechanism, with break age of concrete at the column bases rather than at the column tops.



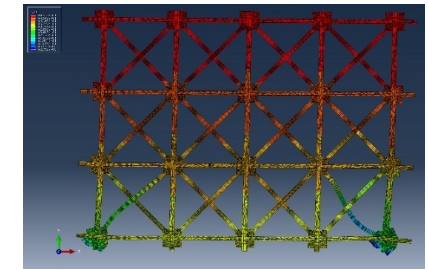
(a)



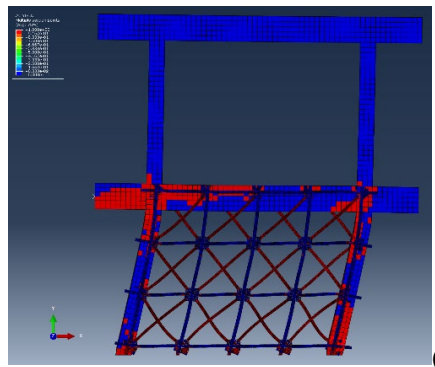
(b)



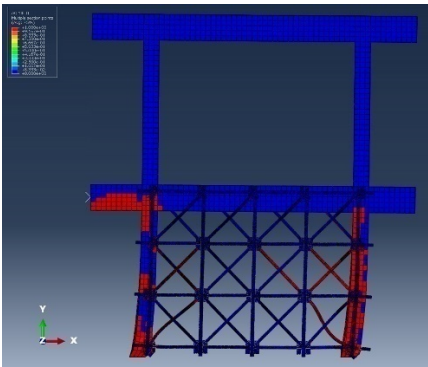
(c)



(d)



(e)



(f)

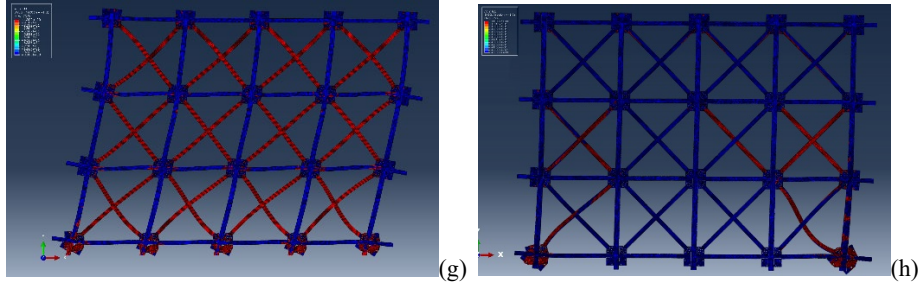


**Fig. 22.** RC Frame + Resisto 5.9 Fixed deformed state (a), RC Frame + Resisto 5.9 NOT Fixed deformed state (b), Resisto 5.9 Fixed deformed state(c), Resisto 5.9 NOT Fixed deformed state (d), RC Frame + Resisto 5.9 Fixed active yield state (e), RC Frame + Resisto 5.9 NOT Fixed active yield state (f), Resisto 5.9 Fixed active yield state (g), Resisto 5.9 NOT Fixed active yield state (h).

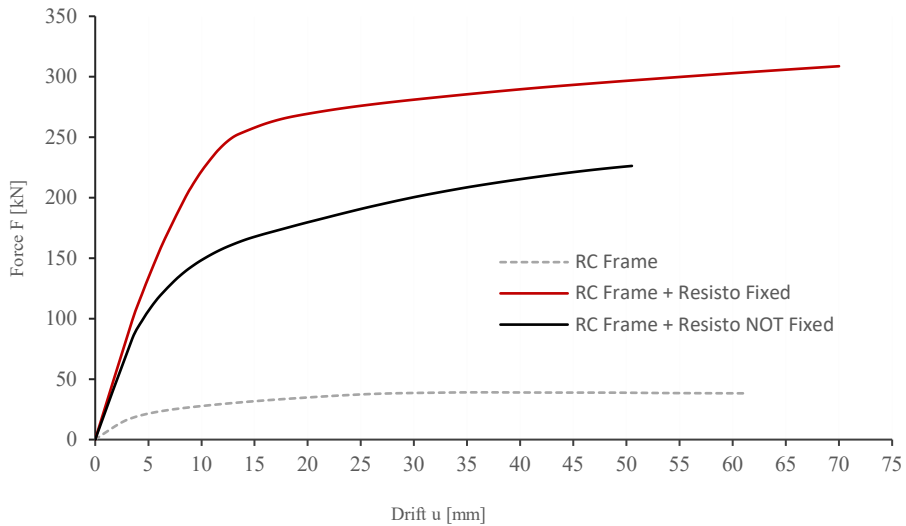


**Fig. 23.** Abaqus pushover curves of the three structural models.

The different behaviour of the two retrofitted FEM models compared to that of the bare RC frame is accurately represented in the pushover curves of **Fig. 23**. Even if the non-fixed model has a worse behavior than the fixed one, it allowed the entire frame to reach stiffness  $K$  and maximum force  $F$  greater than those of the frame without Resisto 5.9. The improving capabilities of the Resisto 5.9 system are displayed from **Table 6** to **Table 8**.

**Table 6.** Displacement (U), Force (F) and Stiffness (K) obtained from the Abaqus pushover curves.

| ID Model                         | U [mm] | F [kN] | K [N/mm] |
|----------------------------------|--------|--------|----------|
| Experimental RC Frame            | 13     | 30     | 5294.80  |
| Numerical RC Frame               | 70     | 39.07  | 5294.80  |
| RC Frame + Resisto 5.9 Not Fixed | 50     | 226.28 | 23966.76 |
| RC Frame + Resisto 5.9 Fixed     | 70     | 308.72 | 25358.62 |

**Table 7.** Percentage increases of the parameters of the numerical RC frame compared to the experimentally tested RC frame.

| ID Model              | U [mm] | F [kN] | K [N/mm] |
|-----------------------|--------|--------|----------|
| Experimental RC Frame | -      | -      | -        |
| Numerical RC Frame    | -      | 30%    | -        |

**Table 8.** Percentage increases of the parameters of the reinforced RC frame compared to the unreinforced RC frame.

| ID Model                         | U [mm] | F [kN] | K [N/mm] |
|----------------------------------|--------|--------|----------|
| RC Frame                         | -      | -      | -        |
| RC Frame + Resisto 5.9 Not Fixed | -      | 479%   | 353%     |
| RC Frame + Resisto 5.9 Fixed     | -      | 690%   | 379%     |
| Fixed – Not Fixed                | -      | 36%    | 6%       |

Since the analyses herein presented were conducted in a displacement-controlled mode, the displacement variation ( $\Delta\%$ ) appears of unnecessary utility. Contrary, in terms of maximum seismic force, the Resisto Not Fixed model was much more resistant (479%) than the bare RC Frame. At the same time, the Resisto Fixed model exhibited a maximum strength very larger than the bare RC Frameone (690%). Percentage differences in terms of stiffness K showed how the Resisto System positively impacts on the investigated RC structure. In particular, an improvement of 353% for the Not Fixed model and 379% for the Fixed one was registered. As a conclusion, the Fixed solution showed a better response than the Not Fixed one both in terms of maximum force (+36%) and stiffness (+6%) due to the different plastic behavior of the two FEM models previously presented.

### 2.10 Pro\_Sap analysis results

The three frames were assessed by means of push-over analyses with concentrated plasticity models. The Pro\_Sap software calculates the limit capacity of plastic hinges according to the assigned sections, materials and load cases. A horizontal force, calculated with a triangular distribution was considered to evaluate the in-plane behaviour of the frames. The pushover curves plot the seismic force (Fb) and the corresponding displacement of the control point (dc) that was assumed at the head of the column. The analyses were performed according to the factors illustrated in **Fig. 24**.

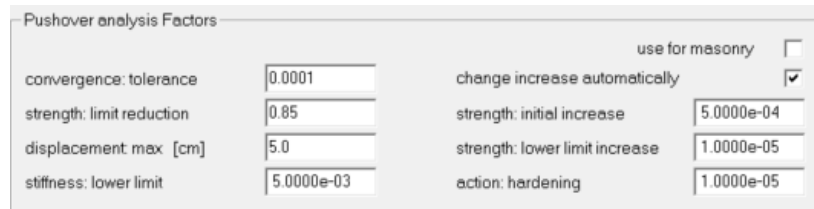


**Fig. 24.** Pushover analysis factors assigned in the Pro\_Sap software.

The comparison between the experimental curve and the numerical curve of the RC frame calculated by means of the Pro\_Sap software is shown in **Fig. 25**, where it is apparent that the two curves showed the same stiffness, but different maximum force.

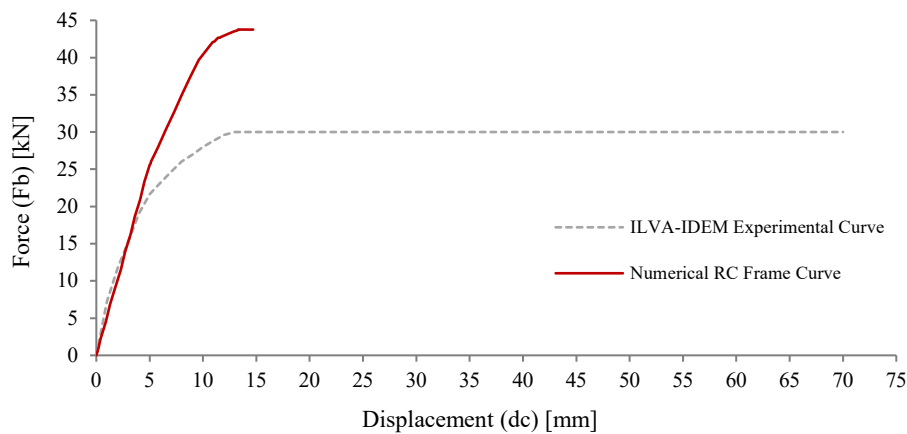


**Fig. 25.** Comparison between experimental curve and numerical one in Pro\_Sap environment referred to the RC Frame.

The results of the pushover curves are depicted in **Fig. 26** and in **Table 9** in terms of maximum force ( $F_{b, \max}$ ), ultimate displacement ( $d_{c, U}$ ), elastic displacement ( $d_y^*$ ) and stiffness ( $K^*$ ) of the equivalent bilinear curve, and ductility ( $\mu = d_{c, U}/d_y^*$ ).

The application of the seismic coating at the first level of the RC frame led to a significant increase of resistance and ultimate displacement, corresponding to equally high increases in stiffness and ductility. The percentage increases of each parameter, compared to the control frame (RC frame) are illustrated in **Table 10**.

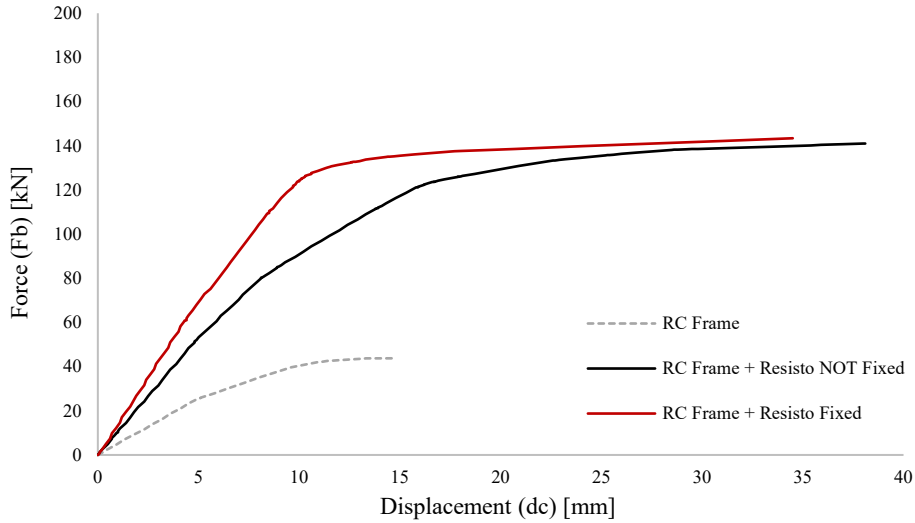


**Fig. 26.** Pushover curves of the three models calculated with Pro\_Sap Software.

**Table 9.** Results of pushover curves of the three models in Pro\_Sap software.

| ID model                     | $F_{b,max}$ [kN] | $d_{c,U}$ [mm] | $d_{y,*}$ [mm] | $K^*$ [N/mm] | $\mu$ [-] |
|------------------------------|------------------|----------------|----------------|--------------|-----------|
| RC Frame                     | 43.76            | 14.7           | 8              | 5033.5       | 1.8       |
| RC Frame + Resisto NOT Fixed | 141.00           | 38.1           | 13.7           | 9576.4       | 2.8       |
| RC Frame + Resisto Fixed     | 143.40           | 34.5           | 10.2           | 13310        | 3.4       |

**Table 10.** Percentage increases of maximum force, ultimate displacement, stiffness, and ductility of the reinforced frames compared to the control one.

| ID model                     | $\Delta F_{b,max}$ | $\Delta d_{c,U}$ | $\Delta K^*$ | $\Delta \mu$ |
|------------------------------|--------------------|------------------|--------------|--------------|
| RC Frame                     | -                  | -                | -            | -            |
| RC Frame + Resisto NOT Fixed | +222%              | +159%            | +90%         | +51%         |
| RC Frame + Resisto Fixed     | +228%              | +135%            | +164%        | +84%         |

Therefore, the seismic behavior of the RC frame was considerably improved thanks to the application of the seismic coating. The fixed boundary conditions (RC Frame + Resisto Fixed) showed a better response to the seismic action in terms of stiffness and ductility with percentage increases of 39% and 22%, respectively, compared to the not fixed solution (RC Frame + Resisto NOT Fixed).

The step-by-step control of the results also allowed to follow the damage evolution of each structural element. In the sections of the RC beam and columns where plastic hinges were assigned, it was possible to assess when plasticization occurred (i.e., the applied moment exceeded the ultimate moment). The results are illustrated in **Fig. 27** for each model with a colored dot representing a plastic rotation value.

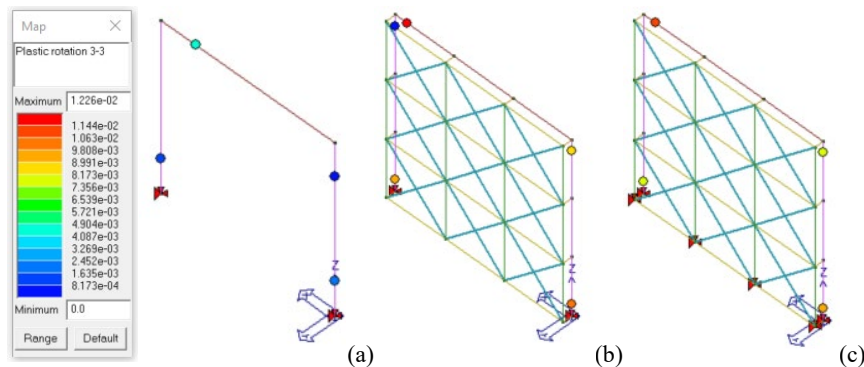


**Fig. 27.** Plastic rotations of RC elements for the three models: RC Frame (a), RC Frame + Resisto NOT Fixed (b) and RC Frame + Resisto Fixed (c).

### 2.11 Comparison between Abaqus and Pro\_Sap results

The comparison between the pushover curves obtained from Abaqus and Pro\_Sap for the three models is illustrated in **Fig. 28**.

The unreinforced RC frame curve showed the same stiffness for both software with a significantly lower ultimate displacement in Pro\_Sap. Both software displayed an increase in base shear and stiffness due to the application of the seismic coating, which is 40-50% higher in Abaqus than in Pro\_Sap. Moreover, Abaqus results show a greater increase in maximum force due to the fixed boundary conditions with a percentage increase of 36%, rather than the increment of 2% of Pro\_Sap's. The differences were found in the necessary approximations made by a more commercial software like Pro\_Sap that manages a limited number of information compared to Abaqus. Some approximations are dependent from the way the software handle the mechanical parameters. Abaqus allows a more precise parametrization of properties, such as plastic behaviour, hardening in high deformations, micro-fracture and so on. This feature allows the software to investigate a higher field of plastic deformations that Pro\_Sap limitedly consider due to its restricted list of editable mechanical parameters. Nonetheless a numerical comparison of the results is described in **Table 11** in terms of maximum force (F) and stiffness (K).

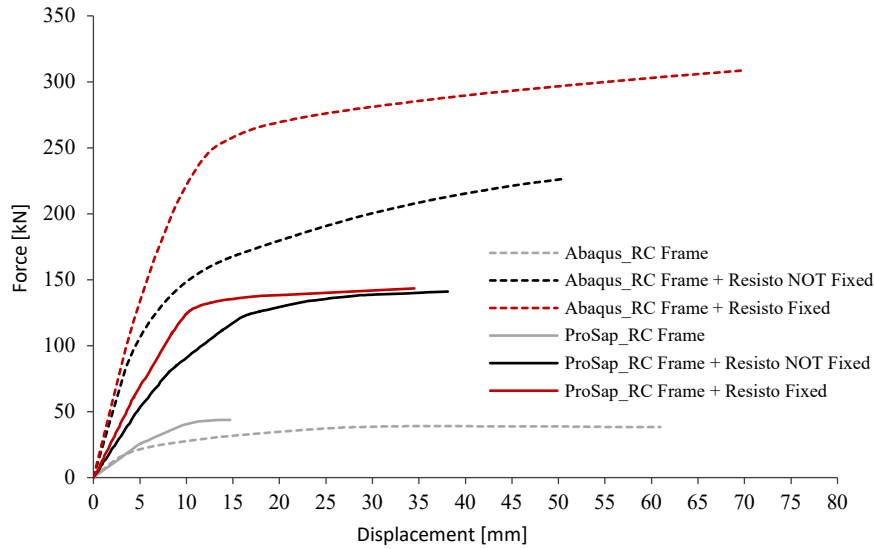


**Fig. 28.** Comparison between Abaqus and Pro\_Sap pushover curves of the three structural models.

**Table 11.** Percentage increases of maximum force and stiffness in the Abaqus models compared to the Pro\_Sap ones.

| ID model                     | $\Delta F_{max}$ | $\Delta K$ |
|------------------------------|------------------|------------|
| RC Frame                     | -12.00%          | +4.94%     |
| RC Frame + Resisto NOT Fixed | +37.69%          | +60.04%    |
| RC Frame + Resisto Fixed     | +53.55%          | +47.51%    |

### 3. Conclusions

The research focused on investigating the application of a cold-formed steel framed exoskeleton to a RC frame extrapolated from an existing building. A plane frame was assessed with and without the reinforcement by means of two structural softwares, namely Abaqus CAE and Pro\_Sap, with the purpose of evaluating the contribution of the seismic coating system and finding the most efficient method to implement the reinforcement in a calculation software. The comparison between these two programs was made with the purpose of assessing the differences in the results of the structures' seismic behaviour, having modelled the same structural sample with two of the most widely used structural softwares. Three structural models were built with the same characteristics in both softwares: a control frame without reinforcement (RC Frame), a reinforced frame with the seismic coat only linked to the RC structure (RC Frame +



Resisto NOT Fixed) and a reinforced frame where the vertical members of the seismic coat are fixed to the foundation structures (RC Frame + Resisto Fixed).

The analyses were carried out by means of a pushover test in both software. The results showed that the seismic coating system provided a significant improvement of seismic performances to the RC frame, especially for the solution with vertical members linked to the foundation system. The contribute of the un-fixed solution (RC Frame + Resisto Not Fixed) was an increase in base shear (479% Abaqus CAE and 222% in Pro\_Sap), ultimate displacement (159% in Pro\_Sap) and stiffness (353% Abaqus CAE and 90% in Pro\_Sap) compared to the RC frame without reinforcement. The fixed solution (RC Frame + Resisto Fixed) showed a better behavior leading to an increase in base shear (690% Abaqus CAE and 228% in Pro\_Sap), ultimate displacement (135% in Pro\_Sap) and stiffness (379% Abaqus CAE and 164% in Pro\_Sap) compared to the RC frame without reinforcement.

The comparison between the results provided from both software showed that, even if the structures were modelled using the same geometrical, mechanical, and loading conditions, the seismic performances obtained from a more commercial calculation software (Pro\_Sap) are significantly worse than the ones obtained from a more accurate software such as Abaqus CAE. Abaqus pushover curves showed higher values of base shear, displacement and stiffness for the reinforced models, suggesting that further analysis should be performed to reduce the gap between these results. However, the necessary approximations of a commercial software allowed to reach the seismic upgrading of the structure by applying the seismic coating system, even if leading to an improvement of the seismic behavior, on the safe side, lower than its potential.

## References

1. G. Di Lorenzo, R. Tartaglia, A. Prota e R. Landolfo, «Design procedure dor orthogonal steel exoskeleton structures for seismic strengthening,» *Engineering Structures*, 2022.
2. U. Saracco, A. Dallari e A. Formisano, «L'uso di Resisto 5.9 per retrofit sismo-energetico di edifici in c.a.,» in *Conferenza Eco-Resis 2022*, Napoli, 2022.
3. G. Di Lorenzo, R. Tartaglia, A. Prota e R. Landolfo, «Design procedure for orthogonal steel exoskeleton structures for seismic strengthening,» *Engineering Structures*, 2022.
4. O. Bellini, A. Marini e C. Passoni, «Adaptive exoskeleton systems for the resilience of the built environment,» *Techne*, 2018.
5. F. M. Mazzolani, *Seismic upgrading of rc buildings by advanced techniques. The ILVA-IDEM researchproject*, Polimettrica, 2006.
6. Certimac, «Rapporto di Prova - RITC\_081\_2022,» 2022.
7. A. Davino, G. Longobardi, E. Meglio, A. Dallari e A. Formisano, «Seismic Energy Upgrading of an Existing Brick Masonry Building by a Cold-Formed Steel Envelope System,» *Buildings*, 2022.
8. P. Sisma, «Resisto 5.9,» [Online]. Available: <https://www.progettosisma.it>.
9. A. Formisano, G. De Matteis e F. M. Mazzolani, «Numerical and experimental behaviour of a full-scale rc structure upgraded with steel and aluminium shear panels,» *Computers and Structures*, 2008.

10. F. M. Mazzolani, G. Della Corte, B. Calderoni, G. De Matteis, B. Faggiano, S. Panico, R. Landolfo e M. Dolce, «The ILVA-IDEM project: full-scale pushover test on existing rc structure - Part I: experimental results» in XI Convegno Nazionale ANIDIS, 2004.
11. F. Mazzolani, «Refurbishment by steelwork» Arcelor Mittal, Luxembourg, 2007.
12. M. D. I. (NTC2018), Norme Tecniche delle Costruzioni, 2018.
13. Dassault Systeme, “Abaqus CAE,” Simulia, [Online]. Available: <https://www.3ds.com/it/>. [Accessed 19 01 2023].
14. 2Si srl, “Pro\_Sap,” [Online]. Available: [https://www.2si.it/it/pro\\_sap/](https://www.2si.it/it/pro_sap/). [Accessed 19 01 2023].
15. A. Formisano, «Seismic upgrade of existing rc buildings by means of metal shear panels: design models and full-scale tests».
16. P. Castaldo, D. Gino, G. C. Marano e G. Mancini, «Aleatory uncertainties with global resistance safety factors for non-linear analyses of slender reinforced concrete columns» Engineering Structures, 2022.
17. D. Gino, P. Castaldo, L. Giordano e G. Mancini, «Model uncertainty in non-linear numerical analyses of slender reinforced concrete members» Structural Concrete, 2021.
18. C. Valente, D. Spina e M. Nicoletti, «Dynamic testing and modal identification» in Seismic upgrading of rc buildings by advanced techniques - The ILVA-IDEM researchproject, Polimetrica, 2006.
19. J. Lubliner, J. Oliver, S. Oller e E. Onate, «A plastic-damage model for concrete» International Journal of Solids and Structures, 1989.
20. Y. Liu e G. Glass, «Effects of mesh density on finite element analysis» SAE International, 2013.
21. A. Dutt, «Effect of mesh size on finite element analysis of beam» SSRG International Journal of Mechanical Engineering, 2015.